phys. stat. sol. (b) 88, 463 (1978)

Subject classification: 6 and 13.1; 20.1

Institute of Semiconductors, Academy of Sciences of the Ukrainian SSR, Kiev

Theory of Cyclotron Resonance of Two-Dimensional Electrons Interacting with Surface and Volume Phonons

By

M. I. DYKMAN

The interaction between nondegenerate two-dimensional electrons in a quantizing transverse magnetic field and volume phonons is shown to be weak for the majority of systems. The coupling to surface phonons often appears to be strong. To separate the contribution of the interaction with volume phonons the diagram technique is developed. The influence of strong and weak interaction with surface phonons on the shape of the absorption peaks near the cyclotron frequency and its overtones and on the dc conductivity is analysed. The dependence of parameters on temperature and magnetic field strength is considered. The transverse electric field is shown to affect the electron–phonon coupling in the case of two-dimensional electrons near semiconductor surfaces.

Показано, что взаимодействие невырожденных двумерных электронов в квантующих магнитных полях с объемными фононами для большинства систем является слабым. Взаимодействие с поверхностными фононами часто может оказаться сильным. Вклад взаимодействия с объемными фононами удается точно выделить в ряде случаев с помощью предложенной в работе диаграммной техники. Проанализировано влияние сильного взаимодействия с поверхностными фононами на форму спектра поглощения на циклотронной частоте и ее обертонах и на статическую проводимость в квантующих магнитных полях. Рассмотрено также слабое одно- и двухфононное взаимодействие. Исследованы полевые и температурные зависимости параметров. Показано, что на константу электрон–фононной связи в случае двумерных электронов у поверхности полупроводников можно влиять электрическим полем.

1. Introduction

At least three types of systems are known where the gas of electrons (holes) is effectively two-dimensional at sufficiently low temperature and concentration: thin films [1, 2], semiconductor surface layers at strong inversion [3], and the liquid He–gaseous He interface [4]. The strong magnetic field parallel to the axis of size quantization turns an energy spectrum of two-dimensional carriers into a discrete one. This results in the change of the character of electron scattering by phonons and impurities which is manifested in cyclotron resonance (CR) and dc conductivity. For example, an intensive absorption near overtones of the cyclotron frequency ω_c by electrons at the Si surface was observed in [5], while in [6] there were observed the strong broadening and shift of the CR peak with the increase in electric field attracting electrons to the liquid helium surface.

In the present paper the isotropic two-dimensional non-degenerate electron gas is considered. The scattering by impurities is neglected. Magnetic fields are supposed to be strong, so that $\omega_c \gg \Gamma$, where Γ denotes the halfwidth of the CR peak. In quantizing fields the scattering by surface and volume phonons is qualitatively different. The electron interacts effectively only with those phonons, whose two-dimensional (parallel to the surface) momentum $\boldsymbol{q}$ is relatively small, $q \lessapprox l^{-1}$ where $l = \sqrt{\hbar/m\omega_c}$

(in the experiments on quantum CR $l \approx 10^{-6}$ cm). Simultaneously the transverse component of the volume phonon momentum may be much greater because it is limited by the reciprocal thickness of the electron layer d_e^{-1}. The inequality $d_e \ll l$ coincides with the condition of two-dimensionality of electrons in case of isotropic electron mass and is supposed to be fulfilled. Hence the wave vectors of the volume phonons coupled to an electron lie in a narrow cylinder in $\boldsymbol{k}$-space. The phonon characteristic frequency $\omega_{ph} = \omega_v$ is determined by the height of the cylinder d_e^{-1} and is high. Therefore, if the interaction parameters are not too large, the coupling to volume phonons is weak: $\omega_v \gg \Omega, \Gamma$, where Ω is the shift of the electron energy levels due to coupling. The shape of the CR peak for weakly coupled electrons was considered in [7, 8]. The broadening of the peak was shown to be due to the electron transitions between Landau levels with emission of phonons. It is small because the number of phonon states at frequency ω_c (or $n\omega_c$, $n > 1$) is sm allif $q \lessapprox l^{-1}$. This is why it seems to be important to investigate the contribution of low-frequency $(\omega(q = 0) = 0)$ surface phonons to the width of the absorption peak (the decay broadening due to the high-frequency surface modes, $\omega(q = 0) \approx \omega_c$, was considered in [8]).

When the scattering is due to surface phonons the inequality $\omega_{ph} = \omega_s = \omega(q = l^{-1}) < \Omega$ may be fulfilled at rather small interaction parameters. The theory of CR of two-dimensional electrons in the case of strong coupling is analogous to some extent to the theory of light absorption by strongly bound impurities [9]. There is, however, an essential difference connected with the degeneracy of the Landau levels due to translational symmetry. The calculation of the CR spectrum is facilitated in the range of relatively high temperatures, $T \gg \hbar\Omega$. This range is very important from the experimental viewpoint and corresponds to helium or hydrogen temperatures because ω_s is small (e.g., in [6] $T/\hbar\omega_s = 200$ for $T = 0.4$ K). The two-phonon interaction and the phonon anharmonicity are also taken into account in the present paper. They are essential in the case of weak coupling to surface phonons.

2. The Shape of the Absorption Peak near the Cyclotron Frequency

When the effective mass approximation is valid the Hamiltonian of the electron–phonon system in quantizing transverse magnetic field may be presented as follows:

$$\left.\begin{aligned} &\mathcal{H} = H_0 + H_1 + H_s; \qquad H_0 = \omega_c p_1 p_{-1}, \qquad p_\alpha = \frac{l}{\sqrt{2}}\left[p_x - i\alpha\left(p_y - \frac{x}{l^2}\right)\right], \\ &\alpha = \pm 1, \qquad [p_{-1}, p_1] = 1, \qquad \hbar = 1, \end{aligned}\right\} \tag{1}$$

$$H_1 = \sum_{\boldsymbol{q}j} \omega_{\boldsymbol{q}j} b^+_{\boldsymbol{q}j} b_{\boldsymbol{q}j} + \sum_{\boldsymbol{q}j} (V_{\boldsymbol{q}j} \exp(i\boldsymbol{q}\cdot\boldsymbol{r})\, b_{\boldsymbol{q}j} + \text{c.c.}), \tag{2}$$

$$\left.\begin{aligned} &H_s = H_s^{(0)} + H_s^{i}, \qquad H_s^{(0)} = \sum_{\boldsymbol{q}} \omega_{\boldsymbol{q}} b^+_{\boldsymbol{q}} b_{\boldsymbol{q}} + \sum_{\boldsymbol{q}_1+\boldsymbol{q}_2+\boldsymbol{q}_3=\boldsymbol{0}} v_{\boldsymbol{q}_1\boldsymbol{q}_2\boldsymbol{q}_3} c_{\boldsymbol{q}_1} c_{\boldsymbol{q}_2} c_{\boldsymbol{q}_3}, \qquad c_{\boldsymbol{q}} = b_{\boldsymbol{q}} + b^+_{-\boldsymbol{q}}, \\ &H_s^{i} = \sum_{\boldsymbol{q}} H_{\boldsymbol{q}} \exp(i\boldsymbol{q}\cdot\boldsymbol{r}), \qquad H_{\boldsymbol{q}} = V_{\boldsymbol{q}} c_{\boldsymbol{q}} + \sum_{\boldsymbol{q}_1} V_{\boldsymbol{q}\boldsymbol{q}_1} c_{\boldsymbol{q}_1} c_{\boldsymbol{q}-\boldsymbol{q}_1}, \end{aligned}\right\} \tag{3}$$

Here the vector potential $\boldsymbol{A}$ is chosen in the form $\boldsymbol{A} = (0, Hx)$; $\boldsymbol{r} = (x, y)$, $\omega_c = |e_0 H|/mc$ (e_0 denotes the electron charge). The Hamiltonian H_1 describes volume and high-frequency surface ($\omega_{0j} \neq 0$) phonons and their interaction with the two-dimensional electron. Index $\boldsymbol{q}$ determines the two-dimensional wave vector of a phonon. Other phonon quantum numbers are specified by j. The anharmonicity for high-frequency modes is not taken into account. For low-frequency surface modes it is supposed to be weak so that $\gamma_{\boldsymbol{q}} \ll \omega_{\boldsymbol{q}}$, where $\gamma_{\boldsymbol{q}}$ is the phonon damping (the anharmonic interaction between surface and volume phonons is discussed later).

The phonon bandwidths are assumed to exceed Ω, Γ. Parameters V in H_s, H_1 are obtained as a result of averaging of the electron–phonon interaction over the width of the electron layer.

Let us consider at first the CR peak shape neglecting anharmonicity and two-phonon interaction. The two-dimensional conductivity of the non-degenerate electrons near the CR peak equals

$$\left.\begin{aligned} &\sigma_{xx}(\omega) = \frac{Ne_0^2\omega_c}{2m\omega} Q(\omega)\,; \qquad Q(\omega) = [\bar{n}(\omega)+1]^{-1}\,\mathrm{Re}\int_0^\infty \mathrm{d}t\,\exp(i\omega t)\,Q(t)\,, \\ &Q(t) = \langle p_{-1}(t)\,p_1(0)\rangle\,, \qquad \omega \approx \omega_c\,, \qquad \bar{n}(\omega) = [\exp(\lambda\omega)-1]^{-1}\,, \qquad \lambda = \frac{1}{T}, \end{aligned}\right\} \tag{4}$$

where N is the electron concentration. The shape of the CR peak is determined by $Q(\omega)$. To calculate $Q(\omega)$ at $\omega_c \gg \Gamma$ it is necessary to determine the time correlation function $Q(t)$ in the large time range $t \gg \omega_c^{-1}$. It is shown in the Appendix that if the condition $\exp(\omega_c/T) \gg 1$ holds, i.e. CR absorption corresponds to the electron transition from the ground to the first excited Landau level, the coupling to volume phonons causes the exponential factor in $Q(t)$. Then $Q(\omega)$ may be presented as

$$Q(\omega) = \frac{1}{\pi}\int \mathrm{d}\omega'\, Q_a(\omega-\omega')\,\frac{\Gamma}{\Gamma^2+(\omega'-P)^2}, \qquad \Gamma = \Gamma_1+\Gamma_0\,, \qquad P = P_1-P_0\,, \tag{4a}$$

where Γ_n and P_n denote the decay width and shift of the n-th level, respectively, (see (A7)). $Q_a(\omega)$ is the spectral distribution of the time correlation function calculated in the adiabatic approximation with regard to the coupling to surface phonons, i.e. neglecting the phonon-induced transitions between Landau levels. Formula (4a) is valid for arbitrary Γ/ω_s. An representation analogous to (4a) may be used also to investigate the shape of the CR spectrum fine-structure lines.[1]) As the shape of a separate line and the shape of $Q(\omega)$ at $\mathrm{e}^{\omega_c/T} \gg 1$ are similar [7], we shall suppose for a while the excited levels to be empty.

The operator of adiabatic coupling $M_0(\boldsymbol{q})$ is the part of the operator $\exp(i\boldsymbol{qr})$ diagonal in the Landau level number (cf. (A3)). As $[M_0(\boldsymbol{q}), M_0(\boldsymbol{q}')] \neq 0$ the two-particle Green's function $G_a(t)$ and its spectral distribution $Q_a(\omega)$ cannot be calculated in closed form for arbitrary interaction strength. To analyse the shape of $Q_a(\omega)$ at strong coupling one may apply the method of moments. In the important case of relatively high temperatures $T \gg \Omega$, ω_s the calculation of moments may be carried out using perturbation theory (in fact only the inequality $T \gg \Omega$ is needed). The first moment determines the "centre of gravity" of $Q_a(\omega)$ and to the first order in Ω/T equals

$$\left.\begin{aligned} &\Omega_1 = \overline{(\omega-\omega_c)} \equiv (I_1)^{-1}\int_{-\infty}^{\infty}(\omega-\omega_c)\,Q_a(\omega)\,\mathrm{d}\omega\,, \quad I_1 = \int_{-\infty}^{\infty} Q_a(\omega)\,\mathrm{d}\omega = \pi\,\langle[p_{-1}, p_1]\rangle = \pi\,, \\ &\Omega_1 \approx \sum_{\boldsymbol{q}} u_{\boldsymbol{q}}^2 l^2 q^2 \left\{1 - \frac{1}{3T}\sum_{\boldsymbol{q}_1} u_{\boldsymbol{q}_1}^2 [1 - \mathrm{j}_0(l^2 q q_1)]\right\}; \qquad u_{\boldsymbol{q}}^2 = \frac{|V_{\boldsymbol{q}}|^2}{\omega_{\boldsymbol{q}}}\exp\left(-\frac{1}{2}\,l^2q^2\right), \end{aligned}\right\} \tag{5}$$

where j_0 is the Bessel function. It appears as a result of averaging $\exp[il^2(q_x q_{1y} - q_{1x}q_y)]$ over the directions of $\boldsymbol{q}$, $\boldsymbol{q}_1$ ($|V_{\boldsymbol{q}}|^2$ is assumed to be independent of the direction of $\boldsymbol{q}$). The term containing this exponential factor corresponds to a diagram with crossing phonon lines.

[1]) The fine structure may appear in the certain temperature range $T \approx \omega_c$ [7] if the non-equidistance of Landau levels exceeds their width substantially. The non-equidistance is connected with both the phonon-induced level shift and the non-parabolicity of the electron energy dispersion law.

The second moment determines the width of $Q_a(\omega)$ and equals

$$\gamma^2 = \overline{(\omega - \omega_c - \Omega_1)^2} \approx$$
$$\approx \tfrac{1}{2} T \sum_{\boldsymbol{q}} u_{\boldsymbol{q}}^2 (lq)^4 - \tfrac{1}{2} \sum_{\boldsymbol{q},\boldsymbol{q}_1} u_{\boldsymbol{q}}^2 u_{\boldsymbol{q}_1}^2 (l^2 q q_1)^2 [1 - j_0(l^2 q q_1)] . \quad (6)$$

The fourth-order terms in (5), (6) contain the typical factor $1 - j_0(l^2 q q_1)$ proportional to the average value of the suitably weighted commutator $[M_0(\boldsymbol{q}), M_0(\boldsymbol{q}_1)]$. It is obvious from (6) that the Landau level degeneracy causes a narrowing of the CR absorption peak as compared with the absorption by an impurity with the same strength of coupling to phonons (in the latter case the terms $\sim (1 - j_0)$ are absent in the expression for γ^2). Probably this narrowing is connected with the following: after the light-induced electron transition not only the phonons adapt to new equilibrium positions but the x-projection of the centre of the cyclotron orbit changes correspondingly.

The third moment of $Q_a(\omega)$ determines the asymmetry of the distribution

$$\sigma_3 = \overline{(\omega - \omega_c - \Omega_1)^3} \approx - T \sum_{\boldsymbol{q},\boldsymbol{q}_1} u_{\boldsymbol{q}}^2 u_{\boldsymbol{q}_1}^2 l^4 q_1^2 [q^2 - q_1^2 (1 - \tfrac{1}{2} l^2 q^2)] +$$
$$+ \tfrac{1}{4} \sum_{\boldsymbol{q}} u_{\boldsymbol{q}}^2 \omega_{\boldsymbol{q}}^2 (lq)^4 + \sum_{\boldsymbol{q},\boldsymbol{q}_1,\boldsymbol{q}_2} (u_{\boldsymbol{q}} u_{\boldsymbol{q}_1} u_{\boldsymbol{q}_2})^2 A(\boldsymbol{q}, \boldsymbol{q}_1, \boldsymbol{q}_2) \quad (7)$$

(the expression for A is cumbersome and will not be presented here). It is clear from (5) to (7) that at $T \gg \Omega_1$ the asymmetry is small, $\sigma_3/\gamma^3 \sim \Omega_1/\gamma \sim \sqrt{\Omega_1/T} < 1$.

When the moments are known one may find $Q_a(\omega)$ using the method of Grame-Sharlier series similar to the theory of Jahn-Teller impurity centres [10]. Even for $T \gg \Omega_1$, $Q_a(\omega)$ appears to be a Gaussian curve with the halfwidth $\gamma\sqrt{2}$ only in a narrow interval $|\omega - \omega_c - \Omega_1| \lessapprox \gamma\sqrt{2}$ near the $Q_a(\omega)$ maximum. The narrowness of the frequency range is due to the absence of a parameter that provides fast convergence of the Grame-Sharlier series. For example, the first correction to Gaussian distribution is proportional [10] to the parameter

$$\frac{\sigma_4}{\gamma^4} - 3 \approx \frac{T^2}{\gamma^4} \sum_{\boldsymbol{q},\boldsymbol{q}_1} u_{\boldsymbol{q}}^2 u_{\boldsymbol{q}_1}^2 \left[l^4 (q^2 - q_1^2)^2 - \frac{1}{4} (l^2 q q_1)^4 \right] [1 - j_0(l^2 q q_1)]$$

of the order of unity (σ_4 denotes the fourth moment of $Q_a(\omega)$). Due to complexity of the expressions for moments and slow convergence of the series it is worth to obtain $Q_a(\omega)$ in this way for the concrete law of the electron–phonon interaction. It should be noticed that the strong coupling $\gamma \gg \omega_s$ may take place at high temperatures even for small Stokes shift, $\Omega_1 \ll \omega_s$ (the theory of strongly coupled impurities is developed for the case $\Omega_1 \gg \gamma, \omega_s$).

If $T > \Omega_1, \omega_s$ and $\Gamma > \omega_s$, then for arbitrary γ/Γ, γ/ω_s the CR peak maximum, according to (5), (A7) lies at the frequency

$$\omega_{m1} = \omega_c + \Omega_1 + P \quad (8)$$

and $Q(\omega)$ is symmetrical. If the decay damping is small, $\Gamma \ll \omega_s$ and $\gamma \leqq \omega_s$, $Q(\omega)$ presents a smooth and broad distribution centred at ω_{m1} (when $T \gg \omega_s, \gamma$) with a singlet out narrow Lorentzian peak at frequency

$$\tilde{\omega}_{m1} = \omega_c + \tilde{\Omega}_1 + P ; \qquad \tilde{\Omega}_1 \approx \sum_{\boldsymbol{q}} u_{\boldsymbol{q}}^2 (lq)^2 (1 - \tfrac{1}{4} l^2 q^2) \quad (9)$$

(the terms of higher order in Ω_1/ω_s are omitted in (9)). The halfwidth of this peak equals Γ, while its intensity contains an exponential factor similar to the Debye-Waller one, and hence it cannot be observed when coupling is strong. If coupling is weak, $\gamma \ll \omega_s$, the CR absorption takes place preferentially in the range of the Lorentzian peak; the adiabatic part of the interaction (3) causes weak phonon sidebands.

For a number of systems (e.g., for thin films) the direct coupling of two-dimensional electrons to volume phonons (2) may be weak and hence it is of interest to analyse $Q(\omega)$ taking into account the coupling to surface phonons only in the case of weak interaction, $\Omega_1, \gamma \ll \omega_s$ and arbitrary T/ω_s. In second order of the interaction (3) $Q(t) \approx \exp(-i\tilde{\omega}_{m1}t)$ at $t \gg \omega_s^{-1}$, i.e. $Q(\omega)$ contains a δ-shaped peak at $\tilde{\omega}_{m1}$. To obtain a finite width of the CR peak it is sufficient to take into account the single-phonon adiabatic interaction in the fourth order (in the case of impurities with non-degenerate energy levels such an interaction does not give a finite width of the zero-phonon line). The broadening is due to non-commutativity of the operators $M_0(\boldsymbol{q})$ and corresponds to elastic scattering of phonons by electron. This scattering causes a damping of the phase of the electron wave function, while the electron energy is conserved. Analogous to the theory of the impurity absorption where such scattering is connected with a direct two-phonon interaction, in what follows this type of the CR peak broadening is called modulational broadening Γ_m. To calculate Γ_m it is convenient to make the canonical transformation in (4)

$$U = \exp\left[-\sum_{\boldsymbol{q}} \frac{V_{\boldsymbol{q}} M_0(\boldsymbol{q})}{\omega_{\boldsymbol{q}}} (b_{\boldsymbol{q}} - b^+_{-\boldsymbol{q}})\right].$$

In the transformed Hamiltonian there appears in particular the term quadratic in $V_{\boldsymbol{q}}$ that describes the scattering of phonons:

$$UH_s^i U^+ = \sum_{\boldsymbol{q}, \boldsymbol{q}_1} \frac{V_{\boldsymbol{q}} V_{\boldsymbol{q}_1}}{2\omega_{\boldsymbol{q}}\omega_{\boldsymbol{q}_1}} (\omega_{\boldsymbol{q}} + \omega_{\boldsymbol{q}_1})\, b^+_{-\boldsymbol{q}} b_{\boldsymbol{q}_1} [M_0(\boldsymbol{q}), M_0(\boldsymbol{q}_1)] + \dots .$$

To second order in this term at $\omega_c > T$ and $t \gg \omega_s^{-1}$,

$$\left.\begin{aligned} &Q(t) = \exp[-i\tilde{\omega}_{m1}t - \Gamma_m t], \quad \gamma, \Gamma_m \ll \omega_s, \\ &\Gamma_m = 2\pi \sum_{\boldsymbol{q}, \boldsymbol{q}_1} u_{\boldsymbol{q}}^2 u_{\boldsymbol{q}_1}^2\, \bar{n}(\omega_{\boldsymbol{q}})[\bar{n}(\omega_{\boldsymbol{q}}) + 1]\, \delta(\omega_{\boldsymbol{q}} - \omega_{\boldsymbol{q}_1})(1 - \tfrac{1}{4} l^2 q^2)^2 (lq)^4 [1 - j_0(l^2 q q_1)]. \end{aligned}\right\} \quad (10)$$

It is clear from (10) that $\Gamma_m \sim T^2$ at $T \lessapprox \omega_s$. At $T \ll \omega_s$ modulational broadening is small.

In the absence of decay broadening the CR spectrum represents the superposition of different (but not distinct, generally speaking) lines corresponding to the light-induced transitions between adjacent Landau levels, for arbitrary ratio between the n-th line modulational broadening $\Gamma_m(n)$ and the level non-equidistance. The non-adiabatic interaction in fourth order of the perturbation theory also makes a contribution to Γ_m, but it appears to be $\sim (\omega_s/\omega_c)^2 \Gamma_m \ll \Gamma_m$. An important contribution to $\Gamma_m(n)$ may be connected with the phonon anharmonicity and the direct two-phonon interaction (3). To second order in $H_{\boldsymbol{q}}$ and v in (3) the modulational broadening $\Gamma_m(n)$ equals

$$\Gamma_m(n) = 4\pi \sum_{\boldsymbol{q}} \sum_{\boldsymbol{q}_1 + \boldsymbol{q}_2 = \boldsymbol{q}} \exp\left(-\frac{1}{2} l^2 q^2\right)\left[L_n\left(\frac{1}{2} l^2 q^2\right) - L_{n+1}\left(\frac{1}{2} l^2 q^2\right)\right]^2 \times$$

$$\times\, \bar{n}(\omega_{\boldsymbol{q}_1})[\bar{n}(\omega_{\boldsymbol{q}_1}) + 1] \left| V_{\boldsymbol{q}\boldsymbol{q}_1} - \frac{6V_{\boldsymbol{q}}}{\omega_{\boldsymbol{q}}} v_{-\boldsymbol{q}\boldsymbol{q}_1\boldsymbol{q}_2} \right|^2 \delta(\omega_{\boldsymbol{q}_1} - \omega_{\boldsymbol{q}_2}) \quad (10a)$$

($L_n(x)$ is Laguerre polynomial). In general all phonons with frequencies $\omega_{\boldsymbol{q}_1} \lessapprox T$ make contributions to $\Gamma_m(n)$ in (10a). If the characteristic frequency $\tilde{\omega}_s$ of the most essential phonons is high, $\tilde{\omega}_s \gg \omega_s, \Gamma_m$, then $q_{1,2} \gg q$ and $|\omega_{\boldsymbol{q}_1} - \omega_{\boldsymbol{q}_2}| \ll \omega_{\boldsymbol{q}_{1,2}} \approx \tilde{\omega}_s$ due to the momentum conservation law. However, the δ-function in (10a) (the energy conservation at phonon scattering) is important if $\Gamma_m \ll \omega_s$. If $\Gamma_m \gtrapprox \omega_s$, the two-phonon coupling is not weak. For intermediate single-phonon coupling, $\gamma \lessapprox \omega_s$, the shape

of the peak centered at ω_{m1} appears to be non-Lorentzian even when $\tilde{\omega}_s \gg \omega_s$ because the modulational broadening contains the contribution of vertical phonon lines that cannot be carried through the lines corresponding to the single-phonon interaction.

The anharmonicity and direct two-phonon interaction cause decay damping of the electron states also, because the inequality $ql \lessapprox 1$ restricts only the total momentum of the phonons participating in a decay process. To second order in v and H_q the decay damping may be described by diagrams similar to those for volume phonons, but now

$$\Gamma_k(q) = 2\pi\left[\bar{n}(|k|\,\omega_c) + \frac{k+|k|}{2|k|}\right]\sum_{q_1+q_2=q}\left|V_{qq_1} - 6V_q v_{-qq_1q_2}\frac{\omega_q}{k^2\omega_c^2}\right|^2 \times$$

$$\times\{[\bar{n}(\omega_{q_1}) + \bar{n}(\omega_{q_2}) + 1]\,\delta(|k|\,\omega_c - \omega_{q_1} - \omega_{q_2}) + 2[\bar{n}(\omega_{q_1}) - \bar{n}(\omega_{q_2})]\,\delta(|k|\,\omega_c + \omega_{q_1} - \omega_{q_2})\} \tag{11}$$

should be substituted into (A5), (A7). It is clear from (10a), (11) that the processes due to the direct two-phonon coupling and to the single-phonon one with the anharmonicity being taken into account, interfere. Since $\omega_c \gg \omega_s$, in (11) $q_{1,2} \gg q$ and therefore $\omega_{q_1} \approx \omega_{q_2} \approx |k|\omega_c/2$ in the first term in curly brackets, while the second term is exponentially small. As far as the range of allowed values of $q_{1,2}$ is narrow ($\sim l^{-1}$) the decay probability (11) is small. Furthermore, in contrast to the modulational broadening, (11) does not contain the large (in the actual temperature range) factor $(T/\omega_s)^2$ and hence makes a small contribution to the CR peak broadening. However, the value of decay damping determines the limits where the theory linear in resonant electric field may be used. If the anharmonicity mixes surface and volume modes the decay of electron energy into energy of volume phonons takes place even in the absence of direct coupling. The damping is described by an expression analogous to (11), but with summation over j.

For the strongly coupled electrons, $\gamma \gg \omega_s$, the influence of weak anharmonicity and two-phonon interaction on $Q(\omega)$ is inessential. For example, these terms do not cause temperature-dependent shift of the CR peak (such a shift appears in the theory of impurity absorption).

3. The CR Overtones and DC Conductivity

To investigate the shape of CR peaks near overtones it is necessary to substitute the complete spectral distribution $\tilde{Q}(\omega)$ into (4) instead of $Q(\omega)$:

$$\tilde{Q}(\omega) = \frac{[\bar{n}(\omega)+1]^{-1}}{2}\sum_{\alpha,\beta=\pm1} Q_{\alpha\beta}(\omega); \qquad Q_{\alpha\beta}(\omega) = \int_{-\infty}^{\infty} dt\, e^{i\omega t}\langle p_\alpha(t)\, p_\beta(0)\rangle\,. \tag{12}$$

Integrating (12) twice by parts and taking into account (1), (3), and (A3) one obtains $Q_{\alpha\beta}(\omega)$ in a convenient form:

$$\left.\begin{aligned} Q_{\alpha\beta}(\omega) = &-(\omega+\alpha\omega_c)^{-1}(\omega-\beta\omega_c)^{-1}\sum_{k,k_1=0,\pm1,\ldots}\sum_{q,q'} l^2 q_\alpha q'_\beta \times \\ &\times\int_{-\infty}^{\infty} dt\, e^{i\omega t}\langle M_k(q,t)\, H_q(t)\, M_{k_1}(q',0)\, H_{q'}(0)\rangle\,, \\ |\omega| \neq \omega_c\,, \qquad q_\alpha = &\frac{1}{\sqrt{2}}(q_x - i\alpha q_y), \qquad M_k(q,t) \sim \exp(ik\omega_c t)\,. \end{aligned}\right\} \tag{13}$$

It is obvious from (4), (12), (13) that the shape of the conductivity peak near $n\omega_c$ is

determined by the term with $k_1 = -k = n$ in (13):

$$\tilde{Q}(\omega) \approx Q_n(\omega)\,, \qquad \omega \approx n\omega_c, \qquad Q_n(\omega) = -\frac{2[\bar{n}(\omega)+1]^{-1}}{(n^2-1)^2\,\omega_c^2} \sum_{\boldsymbol{q},\boldsymbol{q}'} l^2(nq_x + iq_y)(nq'_x - iq'_y) \times$$

$$\times \int_{-\infty}^{\infty} \mathrm{d}t\, \mathrm{e}^{i\omega t} \langle M_{-n}(\boldsymbol{q}, t)\, H_{\boldsymbol{q}}(t)\, M_n(\boldsymbol{q}', 0)\, H_{\boldsymbol{q}'}(0)\rangle\,. \tag{14}$$

When considering overtones ($n \geqq 2$) we shall confine ourselves to the most interesting case of single-phonon interaction with surface modes in the harmonic approximation. The shape of the distribution (14) is qualitatively different for strong and weak coupling. If $\gamma \ll \omega_s$, $Q_n(\omega)$ is a two-humped curve with the gap in the middle and at $\bar{n}(\omega_c) \ll 1$

$$Q_n(\omega) \approx \frac{4\pi(n^2+1)}{n!(n^2-1)^2\,\omega_c^2} \sum_{\boldsymbol{q}} u_{\boldsymbol{q}}^2 \omega_{\boldsymbol{q}} \left(\frac{1}{2} l^2 q^2\right)^{n+1} \{[\bar{n}(\omega_{\boldsymbol{q}})+1]\,\delta(\omega - n\omega_c - \omega_{\boldsymbol{q}}) +$$

$$+ \bar{n}(\omega_{\boldsymbol{q}})\,\delta(\omega - n\omega_c + \omega_{\boldsymbol{q}})\}\,, \qquad \gamma \ll \omega_s\,. \tag{15}$$

At $T \gg \omega_s$ the distribution (15) is symmetrical.

In the case of strong coupling $Q_n(\omega)$ is a single peak whose shape may be investigated at $T \gg \omega_s, \Omega_1$ using the method of moments. The n-th overtone intensity equals

$$I_n = \int_{-\infty}^{\infty} Q_n(\omega)\,\mathrm{d}\omega \approx \frac{8\pi T(n^2+1)}{n!(n^2-1)^2\,\omega_c^2} \sum_{\boldsymbol{q}} u_{\boldsymbol{q}}^2 \left(\frac{1}{2} l^2 q^2\right)^{n+1}. \tag{16}$$

According to (16) $I_n \sim \gamma^2/\omega_c^2 \ll 1$. In the deformation potential approximation (cf. (21)) I_n varies with n slowly, $I_n \sim (n^2+1)/[(n-1)^2\,(n+1)]$ and at $n \gg 1$, $I_n \sim 1/n$, thus the sum of the overtone intensities calculated using (16) diverges. In fact this divergence is unessential, because (14) to (16) are valid only in the case when the overtone peak stands out distinctly from a non-resonance absorption background and hence these expressions cannot be applied to overtones with large n.

The position of the n-th absorption peak centre, $n\omega_c + \Omega_n$, is determined by the first normalized moment of $Q_n(\omega)$. It is approximately independent of temperature at $T \gg \Omega_1, \omega_s$. Although Ω_n and Ω_1 are of the same order of magnitude, there is no simple relation between them valid for arbitrary interaction law. The halfwidth of the n-th overtone peak $\gamma_n \sim \gamma \sim \sqrt{T}$ and in the range of relatively high temperatures the peaks near overtones are symmetrical.

The expressions (4), (12), (13) allow to investigate the dc conductivity of two-dimensional electrons as the CR overtone at zero frequency. It is obvious from (1 that the weak single-phonon coupling in second order of the perturbation theory gives vanishing conductivity $\left(\sum_{\boldsymbol{q}} u_{\boldsymbol{q}}^2 q^2\,\delta(\omega_{\boldsymbol{q}}) = 0\right)$. It is convenient to take account of the higher-order terms by the canonical transformation used to obtain (10). Then to the lowest non-vanishing order

$$\sigma(0) = \frac{Ne_0^2}{m\omega_c T}\,\tilde{\Gamma}_m\,; \qquad \tilde{\Gamma}_m = 4\pi \sum_{\boldsymbol{q},\boldsymbol{q}_1} u_{\boldsymbol{q}}^2 u_{\boldsymbol{q}_1}^2\,\bar{n}(\omega_{\boldsymbol{q}})\,[\bar{n}(\omega_{\boldsymbol{q}})+1] \times$$

$$\times\, l^2 q^2\,[1 - \mathrm{j}_0(l^2 \boldsymbol{q}\boldsymbol{q}_1)]\,\delta(\omega_{\boldsymbol{q}} - \omega_{\boldsymbol{q}_1})\,. \tag{17}$$

The important contribution to dc conductivity of the weakly coupled electrons is connected with the direct two-phonon coupling and the phonon anharmonicity. This contribution is determined by (17) with $\Gamma_m(0)$ from (10a) having been inserted

instead of $\tilde{\Gamma}_m$ (the squared difference of Laguerre polynomials in (10a) should be replaced by $\frac{1}{2}l^2q^2$). Generally speaking, the contributions made by the direct two-phonon interaction and the phonon anharmonicity on the one hand, and by non-commutativity of the operators of the single-phonon coupling on the other hand, interfere. Experimentally these interactions may be distinguished only when the frequencies of essential phonons $\tilde{\omega}_s$ and ω_s are different. If $\tilde{\omega}_s \gg \omega_s$, then at $\tilde{\omega}_s \gg T \gtrless \omega_s$ the main contribution to $\sigma(0)$ is determined by the single-phonon coupling, while at $T \approx \tilde{\omega}_s$ the additional contribution due to $V_{\boldsymbol{q}\boldsymbol{q}_1}$, $v_{\boldsymbol{q}\boldsymbol{q}_1\boldsymbol{q}_2}$ in (3) manifests itself.

In the case of strong coupling we have not succeeded to calculate $\sigma(0)$ directly, but in the temperature range $T \gg \gamma \gg \omega_s$, Ω_0 the conductivity $\sigma(0)$ may be estimated by the method of moments. The function $\omega^{-1}Q_0(\omega)$ has a peak at small (as compared with ω_c, T) frequency Ω_0 with typical halfwidth

$$\left.\begin{aligned} &\gamma_0 = \left[I_0^{-1}\int_{-\infty}^{\infty}(\omega-\Omega_0)^2\,\omega^{-1}Q_0(\omega)\,d\omega\right]^{1/2}, \qquad I_0 = \int_{-\infty}^{\infty}\omega^{-1}Q_0(\omega)\,d\omega \approx 4\pi\Omega_1/\omega_c^2, \\ &\gamma_0^2 \approx 4T\sum_{\boldsymbol{q},\boldsymbol{q}_1} u_{\boldsymbol{q}}^2 u_{\boldsymbol{q}_1}^2 l^2q^2\,[1-j_0(l^2\boldsymbol{q}\boldsymbol{q}_1)]/\Omega_1 . \end{aligned}\right\} \tag{18}$$

If $\gamma_0 \gg \Omega_0$, then $\sigma(0)$ is close to $\sigma(\Omega_0)$ and

$$\sigma(0) = \alpha\frac{2\pi Ne_0^2}{m\omega_c}\frac{\Omega_1}{\gamma_0}, \qquad \alpha \approx 1, \qquad \omega_c > T \gg \gamma \gg \omega_s,\ \Omega_0 . \tag{19}$$

Thus $\sigma(0) \sim T$ for weak coupling and $\sigma(0) \sim T^{-1/2}$ for strong coupling when $\omega_c > T \gg \gamma$.

In the range of higher temperatures, $T \sim \omega_c$, an essential contribution to $\sigma(0)$ may be made by volume phonons. The conductivity is then due to the real phonon-induced transitions between Landau levels. It may be calculated using (4), (12), (13), $H_{\boldsymbol{q}}$ in (13) having been replaced by the interaction (2). To second order of the perturbation theory

$$\begin{aligned} \sigma(0) = {} & \frac{4\pi Ne_0^2}{m\omega_c T[\bar{n}(\omega_c)+1]}\sum_{\boldsymbol{q}}\sum_{k>0}\Gamma_{-k}(\boldsymbol{q})\left(\frac{1}{2}l^2q^2\right)^{k+1}\exp\left(-\frac{1}{2}l^2q^2\right)\times \\ & \times\frac{k^2+1}{(k^2-1)^2}\sum_{n=0}^{\infty}\exp(-\lambda\omega_c n)\frac{n!}{(n+k)!}\left[L_n^k\left(\frac{1}{2}l^2q^2\right)\right]^2 . \end{aligned} \tag{20}$$

Since $\Gamma_{-k}(\boldsymbol{q}) \sim \exp(-k\omega_c\lambda)$ (cf. (A6)) the conductivity (20) is small at $\bar{n}(\omega_c) \ll 1$. The essentially inelastic mechanism of the thermally activated conductivity (20) is an attribute of the system under consideration.

4. Discussion of Results

The theory of the CR spectrum near the cyclotron frequency has much in common with the theory of localized or resonant vibration absorption peak [11, 12] in the case of interaction with volume phonons [7, 8] while in the case of coupling of the electron to surface modes they differ substantially. At the same time the two-dimensional electron dynamics differs from that for three-dimensional electrons strongly coupled to volume acoustic modes in quantizing magnetic fields [13] (in particular a two-dimensional electron is localized in space in a magnetic field even in the absence of coupling to phonons). The conditions of strong coupling may be satisfied rather easily for two-dimensional electrons. We shall estimate the "polaronic" parameter

$\alpha = \Omega_1/\omega_s$ for electrons in semiconductors in the deformation potential approximation

$$|V_q| = S^{-1/2} C \sqrt{\frac{q}{2\varrho\, v_s d}}\,, \qquad \omega_q = v_s q\,. \tag{21}$$

Here S, ϱ, d, and C are the area of the surface, the effective crystal density, the depth of the surface wave penetration, and the "deformation potential", respectively. In general d and C depend on q (for a Rayleigh wave $d \sim q^{-1}$), but to estimate α one may substitute into (21) the values of d and C at $q = l^{-1}$. Having assumed $v_s = 5 \times 10^5$ cm/s, $\varrho = 2.3$ g/cm^3 (the density of Si), $d = 70$ Å, $l = 100$ Å ($H = 62$ kOe, $\omega_s = 3.6$ K), $C = 7$ eV we obtain from (5) $\alpha \approx 4$ and $\alpha \sim \sqrt{H}/d$, i.e. α grows with the increase in magnetic field and with phonons being stronger bound to the surface. However, the strength of coupling in the temperature range $T > \Omega_1, \omega_s$ is determined by the parameter $\tilde{\alpha} = \gamma/\omega_s \approx \sqrt{\alpha T/\omega_s} \sim \sqrt{T/d}H^{-1/4}$, i.e. the coupling appears to become stronger with decreasing magnetic field. This is true if the assumptions $1 \ll \omega_c/\gamma \sim H^{3/4}$ and $1 \ll \omega_c/\omega_s \sim H^{1/2}$ hold and hence at $T \gg \Omega_1, \omega_s$ there exists an optimal range of the field strength where the magneto-polaron effect is manifested most distinctly.

If the characteristic phonon penetration depth $d(l^{-1}) < d_e$ (d_e is the electron layer thickness), the parameter C decreases. For example, choosing the electron wave function in the inversion surface layer in the form [3] $z \exp(-z/2d_e)$ and the phonon one in the form $\exp[-z/d(q)]$ (z denotes the distance from the surface) we obtain the strong dependence of $C(q)$ on $d_e/d(q)$: $C(q) \sim [d(q)/(d_e + d(q))]^3$. The strengthening of the coupling to surface phonons with the increase in the electric field E pressing the inversion layer electrons to the surface may be one of the reasons causing the increase in the CR overtone intensities observed in [5] because d_e and $d(l^{-1})$ are of the same order of magnitude and $d_e \sim E^{-1/3}$ [3]. In fact the condition $C(q) \approx C(0)$ singles out those surface phonons which interact with electrons.

It is evident from the results of the present paper that the self-consistent field approximation used sometimes [14] to consider the two-dimensional electron dynamics in quantizing magnetic fields is incorrect at least for the non-degenerate electrons. In this method the diagrams with crossing lines causing the terms with Bessel functions in (5) to (7), (17) are omitted. These terms are not small. For example, at weak coupling and low temperature $T \ll \omega_s$, one obtains from (17), (21) $\sigma(0) \sim T^8$. The neglect of j_0 in (17) leads to the incorrect dependence $\sigma(0) \sim T^4$. It should be noted also that the CR peak width both for weak and strong coupling differs substantially from the inverse two-dimensional electron momentum relaxation time in the absence of the quantizing magnetic field. These quantities depend differently on temperature and on the coupling parameter.

Appendix

To calculate the correlation function $Q(t)$ in the large time range $t \gg \omega_c^{-1}$ it is convenient to go over to the interaction representation and to perform the averaging over phonons. Then

$$Q(t) = Z_0^{-1} \exp(-i\omega_c t) \sum_{m,n,X,X_1} \sqrt{(n+1)(m+1)}\, \exp(-\lambda\omega_c m) \times$$
$$\times \left(\begin{matrix} n+1, X \\ m, X_1 \end{matrix} \middle| G(t) \middle| \begin{matrix} m+1, X_1 \\ n, X \end{matrix} \right);$$

$$
\left.\begin{aligned}
Z_0 &= \sum_{n,X} \mathrm{e}^{-\lambda\omega_c n} \begin{pmatrix} n, X \\ n, X \end{pmatrix} G(0) \Big| \begin{matrix} n, X \\ n, X \end{matrix} \Big), \qquad \begin{pmatrix} n, X \\ m_1, X' + X_1 - X \end{pmatrix} G(t) \Big| \begin{matrix} n_1, X_1 \\ m, X' \end{matrix} \Big) = \\
&= \sum_{\ldots, m_{\boldsymbol{qj}}, n_{\boldsymbol{qj}}, \ldots} (n, X; m_{\boldsymbol{qj}}| \, U(t, 0) \, |n_1, X_1; n_{\boldsymbol{qj}}) \times \\
&\quad \times (m_1, X' + X_1 - X; n_{\boldsymbol{qj}}| \, U^{-1}(t, -i\lambda) \, |m, X'; m_{\boldsymbol{qj}}) \exp\Big(-\lambda \sum_{\boldsymbol{qj}} \omega_{\boldsymbol{qj}} n_{\boldsymbol{qj}}\Big), \\
&\quad U(t, t') = T \exp\Big[-i \int_{t'}^{t} H_i(\tau) \, \mathrm{d}\tau\Big].
\end{aligned}\right\} \tag{A1}
$$

Here T is the operator of the chronological ordering, $|n_{\boldsymbol{qj}})$ the eigenfunction of the operator $b^+_{\boldsymbol{qj}} b_{\boldsymbol{qj}}$, $|n, X)$ the eigenfunction of the Hamiltonian H_0, $p_\alpha|n, X) = \sqrt{n + (1+\alpha)/2}\, |n+\alpha, X)$ (X defines the x-projection of the cyclotron orbit centre, n is the number of the Landau level). We shall use the diagram technique resembling that by Konstantinov and Perel [15]. Then the lowest-order terms of the expansion of $G(t)$ may be presented as

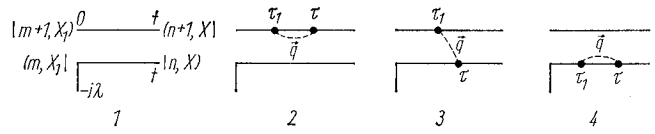

The first diagram (the empty contour) corresponds to the unit operator in the subspace of the electron wave functions. The phonon line connecting the points τ_1 and τ in diagrams 2 and 3 contains the factor

$$
\left.\begin{aligned}
\varphi_{\boldsymbol{q}}(\tau - \tau_1) &= \sum_j |V_{\boldsymbol{qj}}|^2 \, \tilde{\varphi}_{\boldsymbol{qj}}(\tau - \tau_1); \\
\tilde{\varphi}_{\boldsymbol{qj}}(\tau) &= \bar{n}(\omega_{\boldsymbol{qj}}) \exp(i\omega_{\boldsymbol{qj}}\tau) + [\bar{n}(\omega_{\boldsymbol{qj}}) + 1] \exp(-i\omega_{\boldsymbol{qj}}\tau),
\end{aligned}\right\} \tag{A2}
$$

while in diagram 4 the factor equals $\varphi_{\boldsymbol{q}}(\tau_1 - \tau)$ (in the case of surface phonons the summation over j in (A2) should be omitted). When obtaining (A2), the point τ_1 has been supposed to be situated to the left of τ in diagrams 2, 4 and in the upper part of the contour in diagram 3. Each phonon line with momentum $\boldsymbol{q}$ connects two points with momenta $\boldsymbol{q}$ and $-\boldsymbol{q}$. The point with coordinates τ, $\boldsymbol{q}$ corresponds to the electron operator

$$
\left.\begin{aligned}
i^\alpha \mathrm{e}^{i\boldsymbol{q}\boldsymbol{r}(\tau)} &\equiv i^\alpha \sum_{k=0, \pm 1, \ldots} M_k(\boldsymbol{q}, \tau); \qquad (n + m, X| \, M_k(\boldsymbol{q}, 0) \, |n, X') \sim \\
\sim \delta_{k,m} \delta_{X, X' + l^2 q_y} &\exp(-\tfrac{1}{4} l^2 q^2); \quad M_k(\boldsymbol{q}, \tau) = M_k(\boldsymbol{q}, 0) \exp(ik\omega_c \tau); \\
M_k(\boldsymbol{q}, 0) \, M_k(\boldsymbol{q}_1, 0) &= \exp[il^2(q_x q_{1y} - q_{1x} q_y)] \, M_k(\boldsymbol{q}_1, 0) \, M_k(\boldsymbol{q}, 0),
\end{aligned}\right\} \tag{A3}
$$

where $\alpha = 1$ or -1 for the points at the upper or lower part of the contour, respectively.

To obtain the contribution of a diagram to $G(t)$ it is necessary to sum over $\boldsymbol{q}$ in each "arc" (two points with momenta opposite in sign and the phonon line connecting them) and to integrate over coordinates τ_1, τ. The lower limit of the integral over the time-dependent coordinate of a point equals 0 or $-i\lambda$ for points at the upper or lower contour part, respectively, while the upper limit coincides with the time-dependent coordinate of the next to the right point at the same part of the contour. If there is no suitable point to the right, the upper limit of integration equals t. For example, the

diagrams 2 and 3 are equal, respectively, to

$$\left.\begin{aligned} &-\int_0^t d\tau \int_0^\tau d\tau_1 \sum_{k,k_1} \sum_{\boldsymbol{q}} M_k^{\mathrm{u}}(\boldsymbol{q},\tau)\, M_{k_1}^{\mathrm{u}}(-\boldsymbol{q},\tau_1)\, \varphi_{\boldsymbol{q}}(\tau-\tau_1)\,, \\ &-\int_{-i\lambda}^t d\tau \int_0^t d\tau_1 \sum_{k,k_1} \sum_{\boldsymbol{q}} M_k^{\mathrm{d}}(\boldsymbol{q},\tau)\, M_{k_1}^{\mathrm{u}}(-\boldsymbol{q},\tau_1)\, \varphi_{\boldsymbol{q}}(\tau-\tau_1) \end{aligned}\right\} \tag{A4}$$

(the indices u and d specify the operators standing at the upper or lower contour parts). M_k^{u} and M_k^{d} operate on the functions shown near corresponding parts of the contour 1. The $M_k^{\mathrm{u}}(\tau)$ operate one after the other on the "bra-vector" $(n+1, X|$ (in Dirac notations) according to disposition of their points from right to the left (according to the decrease in τ). The $M_k^{\mathrm{d}}(\tau)$ operate on the "ket-vector" $|n, X)$ in the same sequence. The higher-order diagrams for $G(t)$ may be obtained by plotting the corresponding quantity of arcs of types 2, 3, 4 on the contour 1, only topologically inequivalent diagrams being taken into account.

To find the contribution of the coupling to volume phonons to $G(t)$ in the large time range $t \gg \omega_{\mathrm{c}}^{-1}, \omega_{\mathrm{v}}^{-1}$ the fast oscillating character of $\varphi_{\boldsymbol{q}}(\tau-\tau_1)$ at $\tau-\tau_1 \gg \omega_{\mathrm{v}}^{-1}$ should be used. Thanks to such a character the main contribution to the integrals (A4) is given by the time interval $\tau-\tau_1 \approx \omega_{\mathrm{v}}^{-1}$. The main term in the sum over k, k_1 is that with $k=-k_1$ (the rest are fast oscillating ones). These terms being taken into account the asymptotic expression for diagram 2 is of the form

$$-t\sum_{k,\boldsymbol{q}} [\Gamma_k(\boldsymbol{q}) + iP_k(\boldsymbol{q})]\; M_k^{\mathrm{u}}(\boldsymbol{q},t)\, M_{-k}^{\mathrm{u}}(-\boldsymbol{q}, t-0) \sim -\Gamma t\,, \qquad t \gg \omega_{\mathrm{v}}^{-1}, \omega_{\mathrm{c}}^{-1}\,, \tag{A5}$$

where $\Gamma_k(\boldsymbol{q})$ and $P_k(\boldsymbol{q})$ are, respectively, imaginary and real parts of the polarization operator $R(k\omega_{\mathrm{c}} - i0, \boldsymbol{q})$:

$$R(\omega, \boldsymbol{q}) = \sum_j |V_{\boldsymbol{q}j}|^2 \left[\frac{\bar{n}(\omega_{\boldsymbol{q}j})}{\omega+\omega_{\boldsymbol{q}j}} + \frac{\bar{n}(\omega_{\boldsymbol{q}j})+1}{\omega-\omega_{\boldsymbol{q}j}}\right]. \tag{A6}$$

In (A5) Γ denotes the CR peak decay broadening; the point $t-0$ touches the point t from the left.

The time intervals ω_{v}^{-1}, ω_{c}^{-1} are the shortest ones in the problem under consideration. It may be seen from (A4), (A5) that on a reduced time scale, where such intervals are negligible, the points connected by the phonon line in diagrams 2, 4 fit together while in diagram 3 the phonon line becomes practically vertical. Therefore the diagrams with crossing phonon lines or those with one line inside another, arising in higher-order terms of the expansion for $G(t)$, may be neglected as compared with the set of non-crossing diagrams that has the same number of points. Indeed, the contribution of the latter is determined by the integration over a large ($\sim t \gg \omega_{\mathrm{c}}^{-1}$) distance between the arcs. This integration gives a large factor of about t, which compensates the weakness of coupling. In the case of crossing diagrams two (or more) crossing arcs look like a single point on the reduced scale and the large factor due to integration over the distance between the arcs drops. Hence the contribution of these diagrams appears to be of the order of $\Gamma/\omega_{\mathrm{v}}$, $\mathrm{d}\Gamma/\mathrm{d}\omega_{\mathrm{c}} \ll 1$. Analogous arguments may be used to consider the non-adiabatic ($k=-k_1 \neq 0$ in (A4)) interaction with low-frequency surface modes. As $\omega_{\mathrm{c}} \gg \omega_{\mathrm{s}}$, in this case $\Gamma_k(\boldsymbol{q}) = 0$ at $q \lesssim l^{-1}$ and $P_k(\boldsymbol{q}) = |V_{\boldsymbol{q}}|^2\,[2\bar{n}(\omega_{\boldsymbol{q}})+1]/(k\omega_{\mathrm{c}})$.

Consequently if to neglect the adiabatic interaction with low-frequency phonons the diagrams with non-crossing phonon lines only should be taken into account in the perturbation series for $G(t)$. The summation of this series may be easily performed using the obvious inequality $\lambda\Gamma\bar{n}(\omega_{\mathrm{c}}) \ll 1$. Then the equation for $G(t)$ (it is shown by

the thick line) is

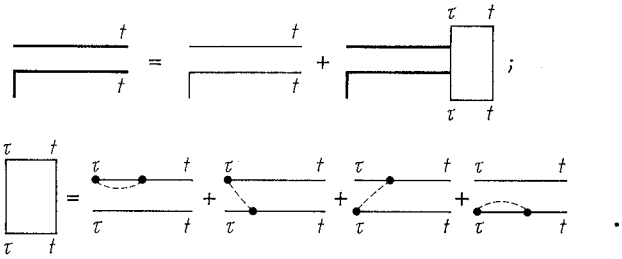

It is necessary to integrate over time here from the left edge up to the point next to the right at any contour part; that is why the diagram 3 has split into two diagrams. Differentiating this equation with respect to t the kinetic equation considered in [8] may be obtained. It contains the terms $M_k^{\mathrm{u}}M_{-k}^{\mathrm{d}}$ which do not appear usually in kinetic equations for systems with discrete energy spectrum. These terms are due to the interference of the decay processes at different Landau levels and are shown to be inessential, if the non-equidistance of the levels exceeds their width substantially [7]. It is obvious from (A1) that they make an exponentially small contribution at $T \ll \omega_{\mathrm{c}}$.

If the adiabatic ($k = k_1 = 0$ in (A4)) coupling to surface modes is important and $\omega_{\mathrm{s}}t \sim 1$, the corresponding diagrams with crossing lines appear to be of the same order as those with non-crossing lines. Nevertheless the diagrams

are proportional to small parameters $\omega_{\mathrm{s}}/\omega_{\mathrm{v}}$, $\omega_{\mathrm{s}}/\omega_{\mathrm{c}} \ll 1$ at $t \sim \omega_{\mathrm{s}}^{-1}$ (here crosses denote operators $M_0(\boldsymbol{q})$, while continuous lines correspond to low-frequency phonons). Thus even the adiabatic coupling being taken into account, the points corresponding to the beginning and the end of a high-frequency phonon line fit together. On the reduced time scale these points coincide and give the operators $M_k^{\mathrm{u}}(\boldsymbol{q}, \tau)\, M_{-k}^{\mathrm{u}}(-\boldsymbol{q}, \tau - 0)$ or $M_k^{\mathrm{d}}(\boldsymbol{q}, \tau)\, M_{-k}^{\mathrm{d}}(-\boldsymbol{q}, \tau - 0)$. These operators commute with each other and with the adiabatic operator $M_0(\boldsymbol{q}, \tau_1)$. This allows to single out immediately the contribution of coupling to high-frequency phonons and non-adiabatic coupling to low-frequency ones when the terms $M_k^{\mathrm{u}}M_{-k}^{\mathrm{d}}(k \neq 0)$ may be neglected:

$$\left.\begin{aligned} \sum_{X_1} \left\langle \begin{matrix} n+1, X \\ m, X_1 \end{matrix} \middle| G(t) \middle| \begin{matrix} m+1, X_1 \\ n, X \end{matrix} \right\rangle &= \delta_{n,m}\, G_{\mathrm{a}}(n, t)\, \mathrm{e}^{-[\Gamma_n + \Gamma_{n+1} + i(P_{n+1} - P_n)]t}, \\ \Gamma_n &= \sum_{k,\boldsymbol{q}} \Gamma_k(\boldsymbol{q})\, |\langle n - k, X + l^2 q_y | M_{-k}(\boldsymbol{q}) | n, X \rangle|^2 . \end{aligned}\right\} \tag{A7}$$

Here Γ_n and P_n are broadening and shift of the n-th Landau level, respectively (the expression for P_n is analogous to that for Γ_n). They are calculated in [7, 8]. The terms with indices n and $n+1$ correspond to operators $M_k^{\mathrm{d}}M_{-k}^{\mathrm{d}}$ and $M_k^{\mathrm{u}}M_{-k}^{\mathrm{u}}$. The function $G_{\mathrm{a}}(n, t)$ is determined by adiabatic coupling to surface modes and does not depend on X. As $[M_0(\boldsymbol{q}, \tau), M_0(\boldsymbol{q}_1, \tau_1)] \neq 0$, we have not succeeded to calculate $G_{\mathrm{a}}(n, t)$ in closed form.

References

[1] I. M. Dykman, Trudy Inst. Fiz. Akad. Nauk Ukr. SSR **5**, 94 (1954).
[2] I. M. Lifshits and A. M. Kosevich, Izv. Akad. Nauk SSSR, Ser. fiz. **19**, 395 (1955).
[3] F. Stern and W. E. Howard, Phys. Rev. **163**, 816 (1967).
[4] V. B. Shikin and Yu. P. Monarkha, Fiz. nizk. Temp. **1**, 957 (1975).
[5] J. P. Kotthaus, G. Abstreiter, and J. F. Koch, Solid State Commun. **15**, 517 (1974).
[6] V. S. Edelman, Zh. eksper. teor. Fiz., Pisma **24**, 510 (1976).
[7] M. I. Dykman, Fiz. tverd. Tela **17**, 3295 (1975).
[8] M. I. Dykman, phys. stat. sol. (b) **74**, 547 (1976).
[9] S. I. Pekar and M. A. Krivoglaz, Trudy Inst. Fiz. Akad. Nauk Ukr. SSR **4**, 37 (1953).
[10] Yu. E. Perlin and B. S. Tsukerblat, Effecty electronno-kolebatelnogo vzaimodeistviya v opticheskikh spektrakh primesnykh paramagnitnykh ionov, Izd. Shtinitsa, Kishinev 1974.
[11] M. I. Dykman and M. A. Krivoglaz, Zh. eksper. teor. Fiz. **64**, 993 (1973).
[12] M. I. Dykman and M. A. Krivoglaz, phys. stat. sol. (b) **68**, 111 (1975).
[13] L. S. Kukushkin, Zh. eksper. teor. Fiz. **57**, 1224 (1969).
[14] V. V. Korneev, Fiz. tverd. Tela **19**, 357 (1977).
[15] O. V. Konstantinov and V. I. Perel, Zh. eksper. teor. Fiz. **39**, 197 (1960).

(Received January 17, 1978)